

Nanopatterning of perovskite manganite thin films by atomic force microscope lithography

Run-Wei Li¹, Teruo Kanki¹, Hide-Aki Tohyama¹,
Motoyuki Hirooka¹, Hidekazu Tanaka^{1,2} and Tomoji Kawai¹

¹ Institute of Scientific and Industrial Research, Osaka University, 8-1 Mihogaoka, Ibaraki, Osaka 567-0047, Japan

² PRESTO, Japan Science and Technology Agency, Japan

Received 10 September 2004, in final form 1 November 2004

Published 30 November 2004

Online at stacks.iop.org/Nano/16/28

Abstract

Atomic force microscopy (AFM) lithography has been performed in $\text{La}_{0.8}\text{Ba}_{0.2}\text{MnO}_3$ (LBMO) films. Unexpectedly, controllable nano-sized patterns can be obtained with an excellent reproducibility under a negative sample bias rather than a positive one, which is completely different from doped SrTiO_3 and high T_C superconductors, though they are of similar perovskite structure. The size of AFM lithography patterns can be controlled well by the sample bias and the selection of tips. Compared to the non-patterned region, AFM lithography patterns exhibit different mechanical, electrical, even possible magnetic properties. Moreover, a simple wet etching can transfer AFM lithography patterns into nano-grooves with a high etching selectivity and without destroying the physical properties of LBMO thin films. It is expected that various spintronic nano-devices will be fabricated with perovskite manganites by AFM lithography and etching techniques.

(Some figures in this article are in colour only in the electronic version)

1. Introduction

Perovskite manganites have attracted increasing interest over the last several years due to their fascinating physical properties, such as colossal magnetoresistance effects, metal–insulator transition and $\sim 100\%$ spin polarization, etc. In particular, lightly doped $\text{La}_{1-x}\text{Ba}_x\text{MnO}_3$ films exhibit extraordinary thickness dependence on the Curie temperature [1–3], so that ferromagnetism remains up to room temperature in an ultrathin film of 50 Å. As a result, lightly doped $\text{La}_{1-x}\text{Ba}_x\text{MnO}_3$ film is considered to be one of the promising candidates for the realization of room-temperature spintronic devices [1]. Undoubtedly, to find a way to fabricate nanostructures in ultrathin perovskite manganite films is considerably important for both fabricating single nanosized spintronic devices and investigating the relevant mesoscopic physics.

In 1990, Dagata *et al* [4] oxidized hydrogen-passivated silicon surfaces using scanning tunnelling microscope (STM). The oxide feature with 100 nm resolution can be used as an etching mask or an insulating barrier. Since then, scanning probe microscope (SPM) lithography has become a highly promising method for nanolithography and the fabrication of nanodevices. It is worth noting that this technique has been extended to the single atomic level, as reported in [5, 6]. On metal [7–12] and semiconductor [13–21] surfaces, nano-patterns have been created by SPM lithography, which has been attributed mainly to an electrochemical oxidation induced by an intense electric field or current. Notably, SPM lithography has been gradually used in perovskite oxides, such as high- T_C superconductors [22–29] and doped SrTiO_3 [30, 31]. The mechanism of SPM lithography in oxides is more complicated. In our previous investigation [31], atomic force microscope (AFM) lithography was successfully performed in Nb-doped SrTiO_3 under a positive sample bias, and relaxation behaviours

of fabricated nanopatterns were observed, which suggests that a significant chemical transport occurs during and after AFM lithography in perovskite oxides.

In this paper, we have investigated AFM lithography in perovskite manganite $\text{La}_{0.8}\text{Ba}_{0.2}\text{MnO}_3$ (LBMO) thin films with the aim of extending AFM lithography into perovskite manganites. It was found that controllable nano-sized patterns could be obtained with excellent reproducibility under a negative sample bias rather than a positive one. The size of AFM lithography patterns could be controlled well by both the sample bias and the selection of tips. Compared to a non-patterned region, AFM lithography patterns exhibited different mechanical, electrical, even possible magnetic properties. A simple wet etching transformed the AFM lithography patterns into nanogrooves with a high etching selectivity. Importantly, AFM lithography and following wet etching did not destroy the important physical properties of LBMO thin films even with a thickness of 100 Å. This finding offers a very important way of fabricating nano-sized spintronic devices with perovskite manganites.

2. Experimental details

LBMO films with a thickness 100 Å were deposited on $\text{SrTiO}_3(100)$ single crystal substrates by laser molecular beam epitaxy in an O_2 atmosphere with a pressure of 0.1 Pa. The substrate temperature was 730 °C. The deposition rate was about 6.3 Å min^{-1} . All the fabricated films were annealed *in situ* with the growth conditions for 20 min and post annealed in 1 atm oxygen at 850 °C for 10 h in order to avoid any oxygen deficiency. The film structure was confirmed by x-ray diffraction. All deposited films indicated atomically flat surfaces. LBMO films were patterned into 10 μm -wide patterns by optical lithography and Ar-ion beam milling. AFM (JEOL JSPM-4200 and DI nanoman) mounted by conductive tips (Si cantilever coated by Pt, Cr-Co alloy, or W_2C) was used to perform AFM lithography with a contact mode in air. During AFM lithography, the tip scanning speed was 500 nm s^{-1} with the feedback on. After the AFM lithography and subsequent wet etching, topologies were observed with tapping or contact mode. Friction force microscopy (FFM) images were obtained by contact mode. The electrical transport properties of patterned nanostructures were measured by means of a physical property measurement system (PPMS).

3. Results and discussion

As is known for SPM lithography processes in metals [7–12], semiconductors [13–21], even in $\text{SrTiO}_{3-\delta}$ [30] and Nd-doped SrTiO_3 [31], a positive sample bias (corresponding to a negative tip bias) is necessary, and no pattern can be obtained under a negative sample bias. At first, we performed AFM lithography on atomically flat LBMO surfaces under a positive sample bias. Mounds and grooves appeared alternately in LBMO films. Usually, the pattern was sub-micron-sized and lacked controllability and repeatability. It seemed to be very difficult to control the size and shape of the pattern though various positive sample biases were tried. However, when a negative sample bias was applied, nano-patterns were obtained with excellent controllability and reproducibility. As

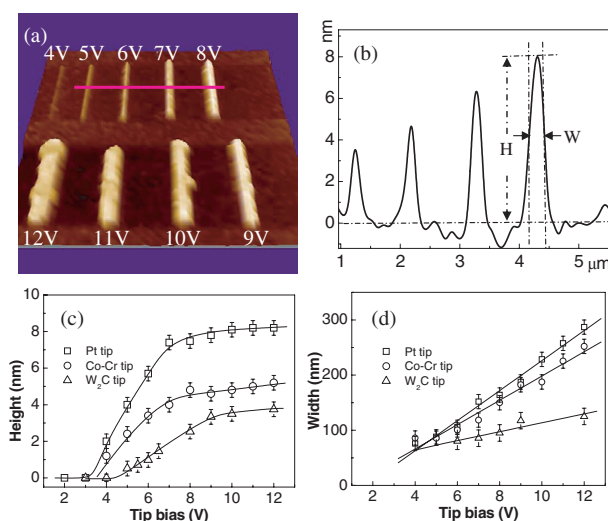


Figure 1. Topography of $\text{La}_{0.8}\text{Ba}_{0.2}\text{MnO}_3$ thin film patterned by AFM lithography with a Pt-coated tip under various negative sample biases (a); cross section (b); tip bias dependence of the height (c) and width (d) of AFM lithography patterns; the tip bias is reversed to sample bias.

a representative, figure 1(a) shows the topography of a LBMO film patterned with a Pt-coated tip under various negative sample biases. The size of the AFM lithography patterns could be well controlled by the sample bias and the selection of tips. The height of the pattern increased with increasing sample bias linearly at first, then saturated at ~ 8 , ~ 5 and ~ 4 nm for the tip coated by Pt, Cr-Co and W_2C , respectively (as shown in figure 1(c)). The threshold voltage, below which the pattern did not appear, was about -4 V for a W_2C -coated tip, and about -3 V for a Pt-coated tip. The width of the AFM lithography patterns also increased linearly with sample bias, and no saturation was observed up to a sample bias of -12 V. Comparing figures 1(c) and (d), one can find that when the sample bias was above a saturation value, which is dependent on the selection of tips, the increase of sample bias only made AFM lithography patterns increase in width, but not in height. Compared to the sample bias and the selection of tips, the reference voltage (which determines the distance or force between tip and sample surface) and tip scanning speed during AFM lithography are not important parameters for controlling the pattern height and width. So far, we have obtained the small patterns with both the pattern width and the interval less than 50 nm by W_2C (as shown in figure 2(c)) or Pt tip.

Figures 2(a) and (b) show the AFM and FFM images of non-patterned LBMO surfaces. Terraced surfaces with the step height of one unit cell size (~ 0.4 nm) can be seen in figure 2(a) and no obvious differences in FFM image. As shown in figure 2(c), by contact mode, five lines were written on the LBMO film surface with a W_2C -coated tip under a sample bias of -8 V. It can be observed clearly in figure 2(d) that these AFM lithography patterns under a negative sample bias were of smaller friction forces compared to the non-patterned region. Because the normal loading force was kept constant during the whole observing process, one can conclude that the friction coefficient of the patterned region was smaller than that of non-patterned regions.

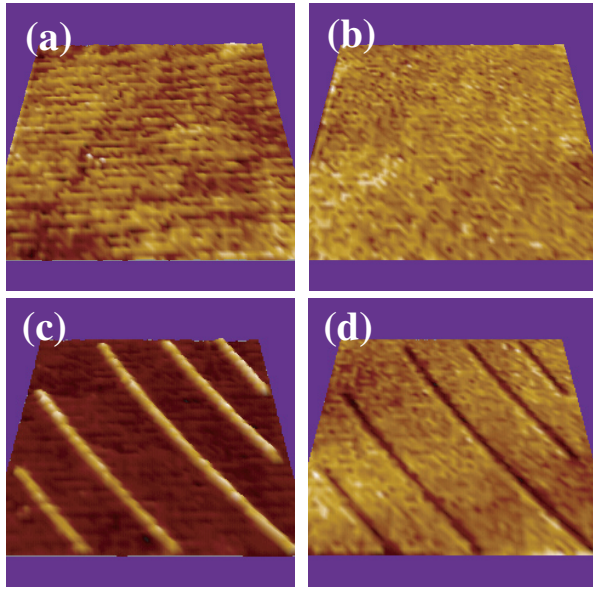


Figure 2. AFM ((a) and (c)) and FFM ((b) and (d)) images of non-patterned $\text{La}_{0.8}\text{Ba}_{0.2}\text{MnO}_3$ surfaces ((a) and (b)) and patterned with a W_2C -coated tip under a sample bias of -8 V ((c) and (d)). The scanning size is $1 \mu\text{m} \times 1 \mu\text{m}$.

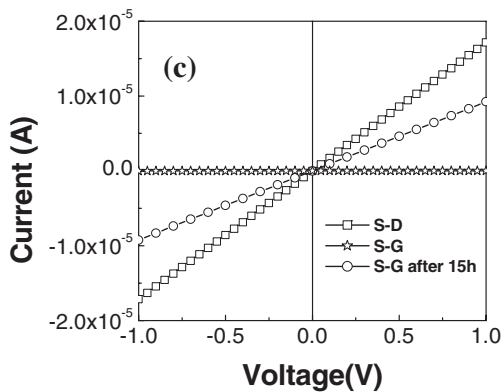
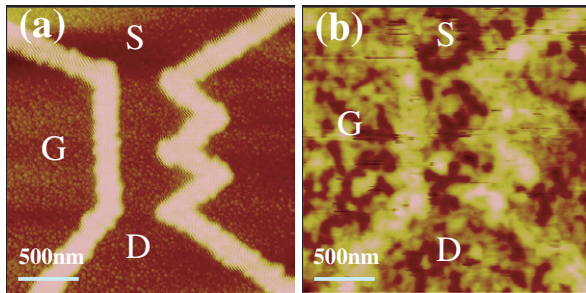


Figure 3. Topographies of the patterned $\text{La}_{0.8}\text{Ba}_{0.2}\text{MnO}_3$ surface under a sample bias of -12 V with a Pt-coated tip measured immediately (a) and 15 h later after AFM lithography (b); current-voltage relationship between electrode S and D, and between electrode S and G (c).

Figure 3(a) shows a structure fabricated under a sample bias of -12 V. The current-voltage characteristics between electrodes S and D, and between electrodes S and G were measured in the voltage range from -1 to 1 V, respectively. As shown in figure 3(c), under a voltage of 1 V, the current was 1.7×10^{-5} A between electrodes S and D, and 1.6×10^{-8} A

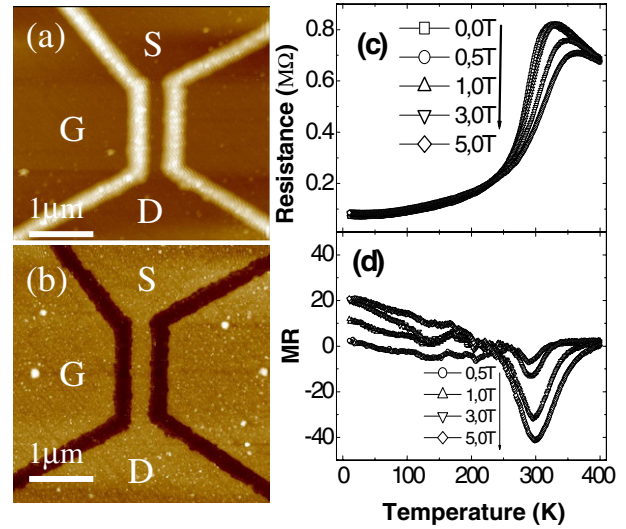


Figure 4. Topologies of a patterned $\text{La}_{0.8}\text{Ba}_{0.2}\text{MnO}_3$ surface (with a Pt-coated tip under a sample bias of -10 V) before (a) and after (b) wet etching. (c) and (d) show the resistance and magnetoresistance of the LBMO channel as a function of the temperature measured under various magnetic fields. The magnetoresistance (MR) was defined as $\text{MR} = \frac{R(H) - R(0)}{R(0)} \times 100\%$ where $R(0)$ and $R(H)$ are the resistance in the absence and in the presence of a magnetic field.

between electrodes S and G. It is suggested that the patterned region was transformed into an insulating barrier, and was of a resistivity three orders of magnitude higher than the non-patterned region. In addition, it is also expected that the magnetism of the patterned region would also be modified by AFM lithography based on the analogy of AFM lithography in Fe_3O_4 thin film [32]. In general, by AFM lithography under a negative sample bias, physical properties, such as mechanical, electrical, and even magnetic properties, could be modulated in nanosized regions.

Similar to that observed in Nb-doped SrTiO_3 single crystal substrates [31], a slow relaxation behaviour of the AFM lithography patterns also appeared in the LBMO films. After laying the sample patterned by AFM lithography in air for 15 h, the patterned lines became obscure (as shown in figure 3(b)), and the resistivity between electrodes S and G became smaller than measured immediately after AFM lithography (as shown in figure 3(c)). The relaxation of the written patterns is obviously disadvantageous if using directly these AFM lithography patterns as insulating barriers. Fortunately, it was found that the introduction of surface defects by Ar bombardment before AFM lithography could stabilize these nanopatterns, which was reported in detail in [31]. Moreover, there are many more defects in the artificial films compared to single crystals. As a result, the relaxation here is much slower than in Nb-doped SrTiO_3 single crystal. On the other hand, the size-controllable patterns obtained under negative sample biases can be easily removed with a high etching selectivity to obtain nano-sized grooves by a few seconds dip in HCl solution. As shown in figure 4(a), two lines were written with Pt-coated tip under a sample bias of -10 V. The patterned sample was dipped in 10% HCl for 15 s. AFM lithography patterns were transferred into grooves. The width and depth of such grooves were ~ 200 nm and ~ 10 nm

(the thickness of the thin film), respectively. The width and depth of grooves could be well controlled by the negative sample bias during the AFM lithography. More importantly, except for the effects caused by the reduction of size, AFM lithography and sequent wet etching did not cause obvious influences on the physical properties of LBMO thin films. This point is very important for fabrication of nanodevices by combining AFM lithography and etching techniques. The resistance as a function of the temperature of the LBMO channel with 200 nm width (see figure 4(b)) was measured under various magnetic fields. As shown in figures 4(c) and (d), a metal–insulator transition appeared at ~ 320 K and a magnetoresistance peak appeared at ~ 300 K, which is basically consistent with that of non-patterned LBMO films [1–3]. In the low temperature range, a positive magnetoresistance appeared, which could be related to the domain wall effects of the sub-micro-sized channel.

4. Summary

In summary, we have realized nano-lithography in $\text{La}_{0.8}\text{Ba}_{0.2}\text{MnO}_3$ films by AFM. It was found that, for the first time, under a negative sample bias rather than a positive one, controllable nano-sized patterns can be obtained with excellent reproducibility and high etching selectivity, which is opposite to that in doped SrTiO_3 though they are of similar perovskite structures. Furthermore, the mechanical, electrical, and even magnetic properties can be modulated with nano-sized resolution by this method. Importantly, AFM lithography and sequent wet etching do not destroy the important physical properties, such as room-temperature ferromagnetism, colossal magnetoresistance effects and metal–insulator transition, of LBMO films even with a thickness of 100 Å. It is expected that various nanodevices, such as spin-field effect transistor [33] and the ferromagnetic single electron transistor, will be fabricated with perovskite manganites by the technology reported here.

Acknowledgment

Thanks to JSPS (Japan Society for the Promotion of Science) for their financial support!

References

- [1] Kanki T, Li R-W, Naitoh Y, Tanaka H, Matsumoto T and Kawai T 2003 *Appl. Phys. Lett.* **83** 1184
- [2] Zhang J, Tanaka H, Kanki T, Choi J-H and Kawai T 2001 *Phys. Rev. B* **64** 184404
- [3] Kanki T, Tanaka H and Kawai T 2001 *Phys. Rev. B* **64** 224418
- [4] Dagata J A, Schneir J, Harary H H, Evans C J, Postek M T and Bennett J 1990 *Appl. Phys. Lett.* **56** 2001
- [5] Sakurai M, Thirstrup C and Aono M 2000 *Phys. Rev. B* **62** 16167
- [6] O'Brien J L, Schofield S R, Simmons M Y, Clark R G, Dzurak A S, Curson N J, Kane B E, McAlpine N S, Hawley M E and Brown G W 2001 *Phys. Rev. B* **64** 161401
- [7] Irmer B, Kehrie M, Lorenz H and Kotthaus J P 1997 *Appl. Phys. Lett.* **71** 1733
- [8] Snow E S and Campbell P M 1995 *Science* **270** 1639
- [9] Snow E S, Park D and Campbell P M 1996 *Appl. Phys. Lett.* **69** 269
- [10] Matsumoto K, Gotoh Y, Maeda T, Dagata J A and Harris J S 2000 *Appl. Phys. Lett.* **76** 239
- [11] Snow E S, Campbell P M, Rendell R W, Buot F A, Park D, Marrian C R K and Magno R 2002 *Appl. Phys. Lett.* **72** 3071
- [12] Wang D, Tsau L and Wang K L 1995 *Appl. Phys. Lett.* **67** 1295
- [13] Snow E S, Campbell P M and McMarr P J 1993 *Appl. Phys. Lett.* **63** 749
- [14] Teuschier T, Mahr K, Miyazaki S, Hundhausen M and Ley L 1995 *Appl. Phys. Lett.* **67** 3144
- [15] Avouris P, Hertel T and Martel R 1997 *Appl. Phys. Lett.* **71** 285
- [16] Held R, Vancura T, Heinzel T, Ensslin K, Holl M and Wegscheider W 1998 *Appl. Phys. Lett.* **73** 262
- [17] Garcia R, Calleja M and Perez-Murano F 1998 *Appl. Phys. Lett.* **72** 2295
- [18] Legr B and Stievenard D 1999 *Appl. Phys. Lett.* **74** 4049
- [19] Tello M and Garcia R 2001 *Appl. Phys. Lett.* **79** 424
- [20] Yang M J, Cheng K A, Yang C H and Culbertson J C 2002 *Appl. Phys. Lett.* **80** 1201
- [21] Bo X Z, Rokhinson L P, Yin H Z, Tsui D C and Sturm J C 2002 *Appl. Phys. Lett.* **81** 3263
- [22] Heyvaert I, Osquiguil E, Van Haesendonck C and Bruynseraede Y 1992 *Appl. Phys. Lett.* **61** 111
- [23] Bertsche G, Clauss W and Kem D P 1996 *Appl. Phys. Lett.* **68** 3632
- [24] Heinzelmann H, Anselmetti D, Wiesendanger R, Güntherodt H J, Kaldis E and Wisard A 1988 *Appl. Phys. Lett.* **53** 2447
- [25] Terashima K, Kondoh M, Takamura Y, Komaki H and Yoshida T 1991 *Appl. Phys. Lett.* **59** 644
- [26] Parks D C, Wang J, Clark N A and Hermann A M 1991 *Appl. Phys. Lett.* **59** 1506
- [27] Thomson R E, Morel J and Roshko A 1994 *Nanotechnology* **5** 57
- [28] Boneberg J, Böhmisch M, Ochmann M and Leiderer P 1997 *Appl. Phys. Lett.* **71** 3805
- [29] Song I, Kim B M and Park G 1997 *Appl. Phys. Lett.* **76** 601
- [30] Pellegrino L, Pallecchi I, Marre D, Bellingeri E and Siri A S 2002 *Appl. Phys. Lett.* **81** 3849
- [31] Li R-W, Kanki T, Tanaka H, Takagi A, Matsumoto T and Tomoji K 2004 *Appl. Phys. Lett.* **84** 2670
- [32] Hirooka M, Tanaka H, Li R-W and Kawai T 2004 *Appl. Phys. Lett.* **85** 1811
- [33] Ahn C H, Triscone J-M and Mannhart J 2003 *Nature* **424** 1015